Vol. 488: 171–185, 2013
doi: 10.3354/meps10382

MARINE ECOLOGY PROGRESS SERIES
Mar Ecol Prog Ser

Published August 15

FREE ACCESS

Upward swimming of competent oyster larvae *Crassostrea virginica* persists in highly turbulent flow as detected by PIV flow subtraction

J. D. Wheeler[1,*], K. R. Helfrich[2], E. J. Anderson[3], B. McGann[3], P. Staats[4], A. E. Wargula[5], K. Wilt[6], L. S. Mullineaux[1]

[1]Department of Biology, Woods Hole Oceanographic Institution, Woods Hole, Massachusetts 02543, USA
[2]Department of Physical Oceanography, Woods Hole Oceanographic Institution, Woods Hole, Massachusetts 02543, USA
[3]Department of Mechanical Engineering, Grove City College, Grove City, Pennysylvania 16127, USA
[4]Department of Electrical and Computer Engineering, Grove City College, Grove City, Pennysylvania 16127, USA
[5]Department of Applied Ocean Physics and Engineering, Woods Hole Oceanographic Institution, Woods Hole, Massachusetts 02543, USA
[6]Division of Biology and Biomedical Sciences, Washington University in St. Louis, St. Louis, Missouri 63110, USA

ABSTRACT: Investigating settlement responses in the transitory period between planktonic and benthic stages of invertebrates helps shape our understanding of larval dispersal and supply, as well as early adult survival. Turbulence is a physical cue that has been shown to induce sinking and potentially settlement responses in mollusc larvae. In this study, we determined the effect of turbulence on vertical swimming velocity and diving responses in competent eastern oyster larvae *Crassostrea virginica*. We quantified the behavioural responses of larvae in a moving flow field by measuring and analyzing larval velocities in a relative framework (where local flow is subtracted away, isolating the behavioural component) in contrast to the more common absolute framework (in which behaviour and advection by the flow are conflated). We achieved this separation by simultaneously and separately tracking individuals and measuring the flow field around them using particle image velocimetry in a grid-stirred turbulence tank. Contrary to our expectations, larvae swam upward even in highly turbulent flow, and the dive response became less frequent. These observations suggest that oyster larvae are stronger swimmers than previously expected and provide evidence that turbulence alone may not always be a sufficient cue for settlement out of the water column. Furthermore, at a population level, absolute velocity distributions differed significantly from isolated larval swimming velocities, a result that held over increasing turbulence levels. The absolute velocity distributions indicated a strong downward swimming or sinking response at high turbulence levels, but this observation was in fact due to downwelling mean flows in the tank within the imaging area. Our results suggest that reliable characterization of larval behaviour in turbulent conditions requires the subtraction of local flow at an individual level, imposing the technical constraint of simultaneous flow and behavioural observations.

KEY WORDS: Turbulence · *Crassostrea virginica* · Settlement · Larval behaviour · Particle image velocimetry

INTRODUCTION

Planktonic larval organisms live in a turbulent ocean environment, and their interactions with this complex physical system have profound impacts on life beyond the small scales at which the interactions occur. Studying the environmental cues that trigger settlement responses in the transitory period between planktonic and benthic stages of invertebrates may be important for our understanding of larval disper-

*Email: jdwhe@mit.edu

sal and supply, as well as early adult survival. Behavioural changes in larvae in response to environmental cues may occur in the benthic boundary layer, allowing larvae to differentiate between microhabitats on the centimetre scale (e.g. Butman 1987, Butman et al. 1988), or higher in the water column. In the water column, behavioural responses may be regulated by temperature, salinity, and light gradients, which operate on larger spatial scales than the localized responses in the bottom boundary layer (for a review, see Metaxas 2001). One such behavioural response is vertical swimming, an important consideration when vertical larval swimming speeds can overcome vertical flow. Self-governed vertical position in the water column affects simulated large-scale dispersal patterns (e.g. Dekshenieks et al. 1996, North et al. 2008) except when vertical mixing is strong (Kim et al. 2010). Vertical position can be especially important for larvae accumulating in vertically sheared flows or fronts, as such flows may facilitate larval transport to nearshore settlement environments (e.g. Helfrich & Pineda 2003, Shanks & Brink 2005, Scotti & Pineda 2007, Woodson et al. 2012) or, under different conditions, act as a barrier (e.g. McCulloch & Shanks 2003, Shanks et al. 2003).

Turbulence is another physical cue that may induce behavioural responses in invertebrate larvae. Given potential strong cross-shore gradients in turbulence, properties of flow may alert larvae as they approach nearshore settlement sites. Downward swimming, sinking, or diving in competent larvae may indicate a behavioural settlement response. In mollusc larvae, such sinking behaviour could potentially be pronounced, as their dense shells impart sinking velocities much greater than their maximum sustained swimming velocities (e.g. Hidu & Haskin 1978). Sinking in high turbulence was reported in Fuchs et al. (2004, 2007) for larval mud snails *Ilyanassa obsoleta*. Such responses are not limited to molluscs: Clay & Grünbaum (2010) reported downward swimming in eight-armed sand dollar plutei in strong shear flows.

We chose to study the eastern oyster *Crassostrea virginica* as their larvae have been observed to regulate vertical position in the water column (Hidu & Haskin 1978, Tamburri et al. 1996) and dive in moderately turbulent channel flows (Finelli & Wethey 2003). Turbulence-mediated recruitment is also a present issue for the conservation of wild oyster populations (Whitman & Reidenbach 2012). Our main objectives were to isolate and quantify the behavioural component of larval vertical velocity (relative to the surrounding flow), determine whether larval vertical velocity varies with turbulence level, and identify the dive response to determine whether it increases in frequency in highly turbulent flow, resulting in a significant change in downward motion of the population as a whole.

The first objective presented a challenging technical problem, in attempting to quantify both larval swimming velocities and local flow velocities simultaneously. Previous experimental studies have investigated invertebrate larval behaviour in grid-stirred turbulence tanks (Fuchs et al. 2004, McDonald 2012, Roy et al. 2012), tank shear flow generated by temperature gradients (Clay & Grünbaum 2010, McDonald 2012), and turbulent flume flows (Hadfield & Koehl 2004, Koehl & Reidenbach 2007, Koehl & Hadfield 2010). Behavioural swimming metrics primarily focused on absolute metrics (without flow subtraction), such as absolute vertical velocity (Roy et al. 2012) and absolute swimming direction (McDonald 2012, Roy et al. 2012). In Fuchs et al. (2004), larval swimming velocities were approximated by mean flow subtraction: average flow velocities from time series were recorded at multiple points in the tank subsequent to larval trials using laser Doppler velocimetry, and these mean flow values were subsequently subtracted from observed larval swimming velocities. In McDonald (2012) and Roy et al. (2012), passive particles of comparable size to the larvae were tracked in an identical experimental set-up to the larval trials, in order to determine differences between swimming in flow and passive advection in flow. These methods of assessing population-level behavioural metrics rely on strict assumptions of spatial and temporal homogeneity of flow, which are likely to be unrealistic and may result in inaccurate estimates of flow near individual larvae and hence erroneous larval behavioural velocities.

We propose that simultaneous tracking of larvae and the surrounding flow is necessary to determine larval behaviour, to fully decouple swimming from advection. This is certainly necessary for identifying individual-level behaviours such as diving, but we further propose that even at a population level, swimming behaviour cannot be discerned from absolute velocity values, instead requiring the local flow to be subtracted from each individual larval trajectory.

Only Clay & Grünbaum (2010) have previously endeavoured to decouple flow from swimming, in a shear flow for sand dollar larvae, by simultaneously tracking passive algae particles in the tank and interpolating the velocity field from the algal trajectories, though they do not report on algal particle density. Our method of determining the flow field, using

particle image velocimetry (PIV), may provide a finer temporal and spatial resolution data set of the recorded flow field.

Further, few grid-stirred tank studies have generated experimental turbulence with energy dissipation rates (ε) consistent with nearshore conditions. Tidal channel and estuarine flows attain dissipation rates ranging from ~10^{-2} to 10^{0} cm^2 s^{-3} (Gross & Nowell 1985), while surf zone conditions range from ε of ~10^{-1} to 10^{2} cm^2 s^{-3} (George et al. 1994). Fuchs et al. (2004) conducted turbulence tank studies with maximum ε of ~2.7 cm^2 s^{-3}, but Roy et al. (2012) and McDonald (2012) set energy dissipation rates more consistent with off-shore continental shelf mixed layers, as they were working with newly hatched and therefore pre-competent sea urchin larvae. In order to address questions of turbulence-mediated settlement effects on oyster larvae, higher turbulence levels are required due to the tendency of these larvae to settle in shallow intertidal and subtidal zones (Kennedy 1996). Although grid-stirred turbulence lacks the strong vertical shear experienced by larvae in a bottom boundary layer, it provides a good system for investigating controlled turbulence in isolation from larger-scale velocity gradients.

The conceptual goal of the present study is to further our understanding of larval oyster settlement behavioural responses in a turbulent water column. We hypothesize that the dive response observed by Finelli & Wethey (2003) is a settlement response that will increase with turbulence in a grid-stirred tank, and that populations of larvae will manifest a downward swimming response (relative to flow) in turbulence through this dive response. Further, we hypothesize that there exists a threshold turbulence level (quantified through energy dissipation rate) above which larvae cease to swim and sink, contributing to a downward velocity response to turbulence.

MATERIALS AND METHODS

Experimental organism

Crassostrea virginica, or eastern oyster, is a species of mollusc found along the Atlantic coast of North America from the Gulf of Mexico to the Canadian Maritimes, and inhabits sub-tidal and intertidal zones in its adult life stage. Spawning occurs in the spring and summer, with a pelagic larval duration of 2 to 3 wk depending on environmental conditions (Kennedy 1986, 1996), although the shell and propulsive velum develop within the first 2 d (Galtsoff 1964). Oyster larvae are competent to settle upon development of eyes and a foot in the pediveliger stage, having shell width exceeding 150–200 µm (Thompson et al. 1996).

Culturing of larvae

Larvae were obtained when near-competent (retained on a 180 µm mesh) from the Aquaculture Research Corporation (ARC), a shellfish hatchery in Dennis, MA, USA. Larvae were maintained in aerated 0.3-µm-filtered seawater (16 l containers) at ambient field surface temperature (20–22°C) and salinity (approximately 33 psu), at densities of ~3000 larvae l^{-1}. Larvae were fed once daily a 375 ml suspension of haptophyte *Isochrysis* sp. in filtered seawater, at an algal density of ~9×10^{5} cells ml^{-1}. Once obtained from the hatchery, larvae were used in turbulence experiments within 2 d to prevent settlement to the bottom of culture buckets. In preliminary experiments, larval shell height at the time of use averaged 220 µm. Larval shell height was not measured for this study, but randomly sampled larvae were examined to ensure the presence of the eyespot and well-developed foot, indicating competency to settle.

Experimental tank

A grid-stirred plexiglass tank (44.5 × 44.5 × 90 cm) was placed in an environmental chamber of fixed temperature (20°C) and filled with 0.3-µm-filtered seawater of ambient field surface temperature (approximately 20°C). Two grids, constructed from 1 × 1 cm plexiglass bars spaced 5 cm apart, were connected equidistantly above and below the experimental field of view, and covered the horizontal cross-section of the tank (Fig. 1). These grids were vertically connected by narrow steel bars and attached to a motor above the tank which oscillated the grids vertically with amplitude 5 cm at a specified frequency. A high-speed monochrome camera (Photron Fastcam SA3) and a pulsed near-infrared laser (Oxford Lasers, Firefly 300 W, 1000 Hz, 808 nm) were trained perpendicularly to illuminate and record a 2.5 × 2.5 cm field of view (FOV) in the centre of the tank, with a laser sheet thickness of approximately 1 mm. A near-infrared laser was used because preliminary experiments with a green laser (532 nm) showed that larvae reacted strongly (dove downward) when exposed to flashes of visible light. The

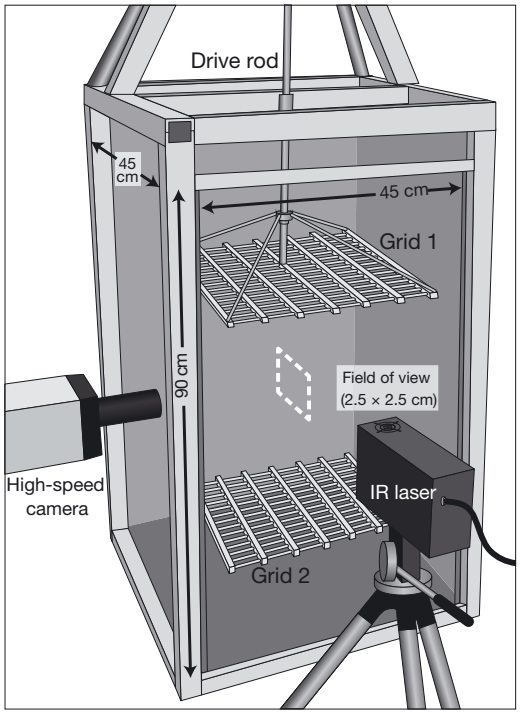

Fig. 1. Experimental tank set-up, with 2 vertically oscillating grids to generate flow and the perpendicularly trained camera and infrared (IR) laser to image a 2.5 × 2.5 cm field of view in the centre of the tank

environmental chamber was therefore kept in darkness for the duration of the experiment.

Experimental procedure

Separate batches of larvae were introduced into the tank as replicates; each batch is identified by a different trial number (T1 through T4). Within each trial, multiple 45 s videos (data sets) were recorded for each turbulence level (or treatment). At the end of each trial, the tank was drained and rinsed, with the larvae discarded. Two separate 2-d experiments (denoted OY5 and OY6) were carried out on different dates, using separate cohorts of larvae from ARC.

Larvae were poured into the tank from a beaker, with numbers ranging from 85 000 to 105 000 larvae (0.5–0.62 larvae ml^{-1}) for each trial. Neutrally buoyant polystyrene particles of 3 to 3.4 µm diameter (Spherotech, 5% weight by volume) in a 2.5 cm^3 suspension volume were injected into the tank to act as passive particles for PIV analysis. Polystyrene particles, rather than natural algae, were necessary to obtain sufficient light scattering for PIV. Although feeding experiments showed that larvae did ingest particles on time scales associated with a single trial (3 h), the ingestion had no significant effect on larval fall velocities. Once particles and larvae were added to the tank, the tank was covered and left undisturbed for 20 min prior to the initialization of a trial, to allow dissipation of flows generated from tank filling and larvae addition. We saw no evidence of the particle-induced behaviours reported by Fuchs et al. (2013), who used 12 µm glass and 20 µm nylon particles, considerably larger than our 3 µm polystyrene particles.

In each trial, treatment order was randomly determined after an initial still water treatment. Still water treatments were conducted at the beginning of each trial due to the difficulties in spinning down the tank completely after higher turbulence treatments. Treatments of increasing turbulence were conducted by oscillating the vertical grid structure at frequencies of 0, 0.25, 0.5, 0.75, 1.25, and 1.75 Hz and a fixed amplitude of 5 cm. These turbulence levels will hereafter be referred to as levels λ_0, $\lambda_{0.25}$, $\lambda_{0.5}$, $\lambda_{0.75}$, $\lambda_{1.25}$, and $\lambda_{1.75}$. In each treatment, data sets were recorded after an initial spin-up time of 5 min to the appropriate turbulence level. Data sets corresponded to approximately 45 s of footage at 60 frames per second (fps). Approximately 5 min elapsed between the recording of each data set, due to data transfer times between the camera and hard drive. In experiment OY5, 4 data sets were recorded for each treatment, up to $\lambda_{1.25}$. In OY6, the number of data sets was adjusted to improve the number of larval tracks, based on observations from OY5. The number of data sets in OY6 was 5, 5, 5, 4, 3 and 4, respectively, for turbulence levels from λ_0 to $\lambda_{1.75}$. The $\lambda_{1.75}$ turbulence level was added in OY6.

For all treatments, the camera recorded images at 60 fps. For treatments up to turbulence level $\lambda_{0.75}$, the laser flashed at 60 Hz, while at higher turbulence ($\lambda_{1.25}$ and $\lambda_{1.75}$) a frame straddling method was employed between the camera and the laser, where the camera triggered the laser to delay and then pulse for brief intervals during the recording, effectively creating successive pairs of images having long and short time steps. All high-turbulence analysis was conducted on the short time step image pairs, to facilitate correlation of passive particle position during PIV analysis (see 'Quantification of flow field and isolation of larval swimming', below). These time steps were 0.0075, 0.008, and 0.006 s^{-1} for OY5 $\lambda_{1.25}$, OY6 $\lambda_{1.25}$, and OY6 $\lambda_{1.75}$, respectively. Relevant experimental values (grid frequencies, numbers of data sets, and time steps) are summarized in Table 1. Experimental images from each data set were saved as high-resolution (1024 × 1024 pixels) TIFF files and subjected to analysis for larval tracking and flow visualization.

Table 1. Detail of experimental setup for each turbulence level. Grid frequency is the rate of vertical oscillation of double grids. Data sets are the replicate trials in experiments OY5 and OY6. Time step is the time delay between 2 paired particle image velocimetry images. Dissipation rate ε calculated as in Doron et al. (2001)

Turb. level	Grid frequency (Hz)	No. data sets	Time step (s^{-1})	ε ($cm^2\ s^{-3}$)
λ_0	0	4 (OY5), 5 (OY6)	0.0167	→0
$\lambda_{0.25}$	0.25	4 (OY5), 5 (OY6)	0.0167	0.002
$\lambda_{0.5}$	0.5	4 (OY5), 5 (OY6)	0.0167	0.017
$\lambda_{0.75}$	0.75	4 (OY5), 4 (OY6)	0.0167	0.064
$\lambda_{1.25}$	1.25	4 (OY5), 3 (OY6)	0.0075 (OY5), 0.008 (OY6)	0.373
$\lambda_{1.75}$	1.75	0 (OY5), 4 (OY6)	0.006	0.667

Data analysis

Individual larval velocity in flow is composed from the sum of both larval swimming and advection by the flow field. We denote individual vertical larval swimming velocity as w_s, and vertical local flow velocity as w_f, so that the absolute vertical larval velocity (w_a) observed for an individual is:

$$w_a = w_s + w_f$$

In the absence of a well-resolved flow field in space, as would occur in the absence of PIV data, one could approximate w_f with a temporal average $\langle w_f \rangle$ at a point or set of points in space. We denote larval vertical swimming velocities calculated using this approximation as mean-shifted swimming velocities, or w_{ms}:

$$w_{ms} = w_a - \langle w_f \rangle$$

We will assess the validity of this spatial and temporal flow field averaging when isolating larval swimming velocities to determine whether simultaneous quantification of flow and larval swimming is necessary.

The methods by which these values are determined experimentally are addressed in the following 2 subsections. Two further subsections address the identification of the dive response in larval trajectories and the method by which the energy dissipation rate is calculated for a given turbulence level.

Larval tracking

Absolute vertical larval velocities w_a were obtained using the following larval tracking procedure. All TIFF images were filtered to remove average background intensity and passive particles (prior to filtering, images were predominantly black with larvae appearing as white spots and smaller passive particles appearing as a pale haze) using LabVIEW 2010 (National Instruments) software. Centroid positions (x and z coordinates) of larvae were identified using the software, along with body size and frame number in which they were identified. An in-house MATLAB (v.7.12.0 R2011a) code was developed to track each individual larva from frame to frame, according to a user-specified tolerance radius in which the larva could be found in a subsequent frame. Larval tracks were identified using this method. All tracks of fewer than 5 frames in length were discarded (usually due to the larva passing out of the FOV too quickly). Instantaneous velocities were then calculated from larval positions in each pair of frames to obtain individual absolute vertical larval velocities, w_a.

Quantification of flow field and isolation of larval swimming

Local flow fields were quantified using the following PIV methodology to calculate vertical flow velocities (w_f) local to each larva. Experimental TIFF files were first imported into LaVision DaVis (v.7.2) imaging software. Each experimental image or frame showed the entire FOV for a given time step. For $\lambda_{1.25}$ and $\lambda_{1.75}$, the frames were grouped 1+2, 3+4, etc. prior to analysis due to frame straddling in the camera/laser set-up. Each frame was subdivided into final interrogation windows of 16 × 16 pixels (multi-pass interrogation with no overlap), and cross-correlations were computed between the particles in the interrogation window and in shifting search windows in the next frame, to determine the most probable location of the same particles in the next frame. We used the DaVis default FFT with Whittaker reconstruction as the correlation function. For a given data set, the PIV analysis generated two 64 × 64 matrices for each time step, corresponding to the horizontal and vertical flow velocities on a grid in the FOV (Fig. 2), with a spatial resolution of 0.039 cm between grid points.

These velocity fields were converted into MATLAB data files, and were integrated into the larval tracking code. Each larval position identified a dynamic annulus with an inner radius corresponding to the

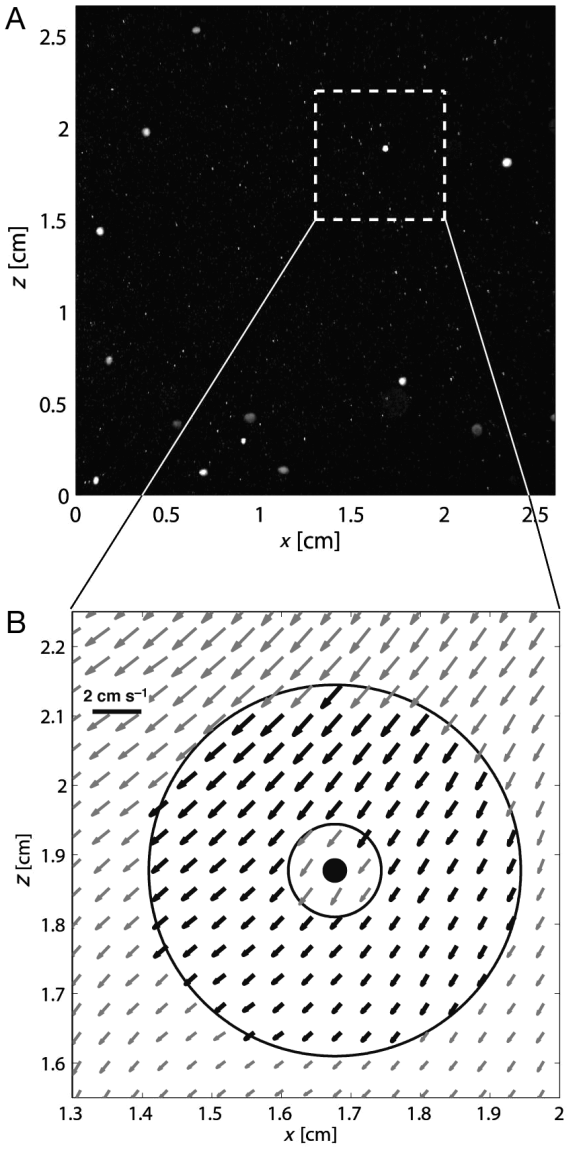

Fig. 2. (A) Image of field of view in turbulence tank, where eastern oyster larvae are bright white spots and passive particles are smaller specks. Large diffuse spots are out-of-focus larvae (filtered out prior to analysis). (B) The enlarged image is a sample velocity field determined from particle image velocimetry analysis, where the larva is the black circle, and all black velocity vectors fall within the annulus by which local flow velocity w_f was calculated for the given larva

sum of 2 values: the maximum larval radius in the data set and the PIV spatial grid interval. The outer radius was 4 times greater than the inner radius (Fig. 2). Such an annulus was selected to account for blurring and poor PIV results in the larval boundary layer. Further, the flow very close to the larva would be subject to larval propulsion and wake, and we wished to avoid this bias to the local flow. Results were not sensitive to the outer radius of the annulus, as the flow remained coherent for 6 to 8 PIV velocity vectors away from the larva. Within the annulus for each larva in each frame, the mean vertical velocity from the PIV analysis was computed, and this mean velocity was identified as the local vertical flow velocity around the larva, w_f. For each larva in each frame, larval swimming velocities (w_s) were obtained from $w_s = w_a - w_f$.

The flow data from the PIV analysis were also used to determine the average flow velocity in each data set. The centre points of each quadrant in the FOV were selected and the flow velocity time series of each data set was extracted from the PIV data (Fig. 3). The average flow velocity in the FOV was calculated from these 4 time series for each data set to give $\langle w_f \rangle$, and the mean-shifted larval swimming velocities were obtained from $w_{ms} = w_a - \langle w_f \rangle$.

Identification of dive response

The dive response was identified in larval tracks through extensive comparison of experimental footage and corresponding individual swimming velocity time series. Through visual identification of the dive response in the experimental footage, we found a corresponding signature in the time series data, comprising of a sudden (within 1–2 time steps) drop in vertical velocity to swimming velocities in the range of −0.4 to −0.8 cm s^{-1}. The larval descent would then slow over 10–20 time steps before the vertical velocity would stabilize. Larval trajectories were classified as dive response tracks if they reached accelerations of 3.0 cm s^{-2} (approximately 150 body lengths s^{-2}) for more than one time step, and achieved negative vertical velocities of at least −0.4 cm s^{-1}.

Calculation of turbulent energy dissipation rate

Energy dissipation was estimated through a separate set of PIV-only experiments in the same grid-stirred turbulence tank. These tests employed a green Nd/Yag laser (Big Sky) and a LaVision Imager Pro X camera (2048 × 2048 pixels). Spherical® 10 µm hollow glass spheres were used as the tracer particles in 3-µm-filtered seawater. The image FOV was 12 × 12 cm, centred in the tank. At each turbulence level, 3 sequences of 150 image pairs were acquired at 4 Hz for later PIV analysis using LaVision DaVis PIV software. The inter-frame time was adjusted between turbulence levels for optimal PIV analysis. Velocity vectors were computed using 32 × 32 pixel interroga-

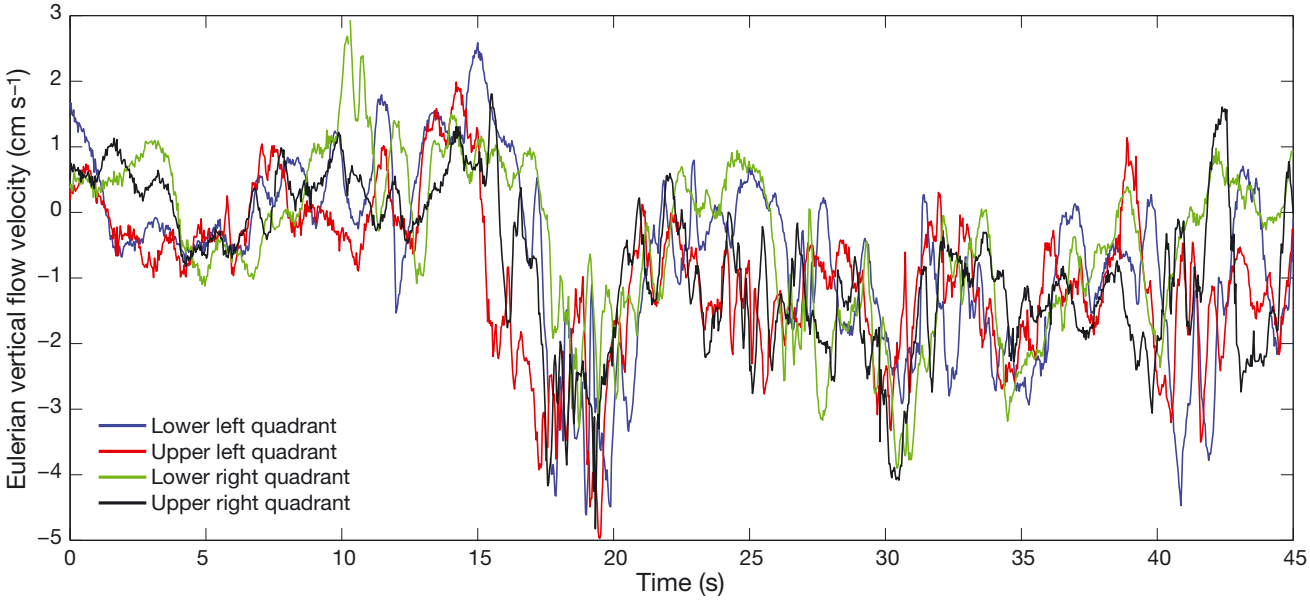

Fig. 3. Vertical velocity time series at central points in the 4 quadrants of the field of view, selected from a level $\lambda_{1.25}$ data set in OY5, used to calculate the temporal average of vertical local flow velocity, $\langle w_f \rangle$

tion regions with 50% overlap, resulting in 128 × 128 vectors with separation of 0.119 cm. Dissipation rates (ε) were calculated directly from the 2-dimensional vector fields from Doron et al. (2001):

$$\varepsilon = 3\nu\left[\overline{\left(\frac{\partial u}{\partial x}\right)^2} + \overline{\left(\frac{\partial u}{\partial z}\right)^2} + \overline{\left(\frac{\partial w}{\partial x}\right)^2} + \overline{\left(\frac{\partial w}{\partial z}\right)^2} + 2\overline{\left(\frac{\partial u}{\partial z}\frac{\partial w}{\partial x}\right)} + \frac{2}{3}\overline{\left(\frac{\partial u}{\partial x}\frac{\partial w}{\partial z}\right)}\right]$$

Here u and w are velocities in the horizontal, x, and vertical, z, directions, respectively, and ν is the kinematic viscosity of seawater. The overbar indicates a mean over the FOV and time at a fixed turbulence level. Prior to computing ε the individual vector fields were passed through a median filter and the derivatives were then estimated using least-squares finite difference stencils to reduce noise (see Raffel et al. 1998). Since the flow is inherently 3-dimensional, the estimate of dissipation rate from 2-dimensional velocity fields assumes that the turbulence is isotropic and that the out of plane, y-direction, velocity fluctuations (v) have average magnitudes equal to the in-plane values (see Doron et al. 2001). These criteria are not precisely met in a grid-driven flow. However, the symmetry of the grid implies that $u \sim v$. Furthermore, the measurements show that the ratio of w_{rms} to u_{rms} of root-mean-squared values is order 1, ranging from ≈2 to 1 from the lowest to highest turbulence levels considered. This anisotropy is typical of grid-forced turbulence. The central location of the FOV between grids promotes homogeneity of the turbulence.

Statistical analysis

The primary objective of this paper was to determine differences between larval vertical swimming velocities in varying levels of turbulent flow. However, prior to this analysis, differences between absolute and larval swimming velocity distributions in each turbulence level were determined to examine the robustness of previous methodologies in decoupling larval behaviour from flow. Distributions of larval velocities (denoted by W and an appropriate subscript) are constructed by combining all individual instantaneous velocities, so that W_s, for instance, is the distribution of larval swimming velocities w_s, for a given turbulence level. Statistical analyses were carried out to compare larval swimming velocity distributions W_s, calculated by our PIV methods with the more typically used mean-shifted swimming velocity distributions, W_{ms}. We also determined statistical differences between larval swimming distributions W_s over increasing turbulence levels. Finally, we determined the statistical significance of changes in dive frequency with respect to turbulence level. Because of the non-independence of the data in the distributions (velocity of a larva at time step t is likely correlated to velocity in nearby time steps), all statistical analyses were conducted on the mean instantaneous velocity of each larval track. All statistical analyses, unless otherwise referenced, were carried out using MATLAB statistical routines at a significance level of $\alpha = 0.05$ with the appropriate Bonferroni correction.

For each trial in each turbulence level, we compared the means and the variances of the mean-shifted swimming velocity distribution (W_{ms}) and isolated swimming velocity distribution (W_s), using a modified 2-tailed *t*-test (Welch's approximate *t*-test statistic and Satterthwaite's approximation for the degrees of freedom) for means and the 2-tailed variance ratio test for the variances.

To determine the effect of turbulence level on the mean vertical swimming velocity, and also the effect of turbulence treatment order, we conducted a 2-way ANOVA. Significance levels in ANOVAs can be adversely affected by the combined effects of heterogeneity of variance and sample size, but the effect of non-homoscedasticity on the ANOVA's significance level is almost negligible when sample sizes are equal (Glass et al. 1972). We therefore sub-sampled the distributions in each turbulence level and trial so the sample size in each matched the smallest sample in the initial set. Though the larval population in the tank remained the same within a trial for the different turbulence levels, the experimental design does not call for a repeated-measures analysis, as the large quantity of larvae in the tank and frequent mixing suggests that resampling of larvae in the FOV was rare. Two subsequent tests were implemented in the case of a significant ANOVA result. First, multiple comparisons of the mean swimming velocities in the different turbulence levels were carried out using Tukey-Kramer's honestly significant difference criterion, and second, 1-tailed *t*-tests were implemented to determine whether vertical directional swimming was significantly different from zero for each turbulence level. These 2 sets of tests are complementary, as the *t*-test compares larval swimming with a zero velocity baseline while the multiple comparison test examines the differences in swimming velocity between turbulence levels.

Dive frequencies were compared between turbulence levels using a χ^2 binomial comparison test with Yates' corrected χ^2 test statistic (Yates 1934), to determine whether the proportion of larvae that dove was dependent on the turbulence level. The contingency tables of the binomial comparison test were then subdivided to identify the turbulence threshold at which a significant difference in dive frequency was detected.

RESULTS

Energy dissipation rate

Using a kinematic viscosity of $\nu = 0.01$ cm^2 s^{-1} for seawater, we found the following energy dissipation rates ε for the experimental turbulence levels: $\varepsilon_{\lambda 0} \rightarrow 0$, $\varepsilon_{\lambda 0.25} = 0.002$, $\varepsilon_{\lambda 0.5} = 0.017$, $\varepsilon_{\lambda 0.75} = 0.064$, $\varepsilon_{\lambda 1.25} = 0.373$, and $\varepsilon_{\lambda 1.75} = 0.667$ cm^2 s^{-3} (where λ denotes the grid oscillation frequency; Table 1). This range of dissipation rates is consistent with those recorded in tidal channels, estuaries, and calmer surf zones (Gross & Nowell 1985, George et al. 1994), and therefore suitable for testing oyster larvae settlement responses. The Kolmogorov length scale at the highest experimental turbulence level (0.035 cm) is comparable to the spatial resolution of the PIV data (0.039 cm), and so we capture the smallest-scale flow dynamics in the turbulence tank.

Absolute versus isolated vertical swimming velocity

In all turbulence levels except λ_0 and $\lambda_{0.25}$, the variances of the mean-shifted swimming velocity distributions and swimming velocity distributions (W_{ms} versus W_s) differed significantly in all trials. At λ_0, where no flow was induced in the tank, the variances in W_{ms} and W_s were not significantly different in 5 of the 8 trials, and at $\lambda_{0.25}$, the variances were indistinguishable in 1 of 8 trials (Table 2). At all other turbulence levels, the variances of these 2 distributions were significantly different in all trials (8 of 8 at $\lambda_{0.50}$–$\lambda_{1.25}$ and 4 of 4 at $\lambda_{1.75}$). Clearly, the variance of the larval swimming velocity distribution cannot be captured by the mean-shifted velocity distribution when even weak flow is induced in the tank.

The means of the 2 distributions were also compared for each trial, at each turbulence level. The means of the 2 distributions were statistically different in no trials at λ_0, in 2 of 8 trials at $\lambda_{0.25}$ and $\lambda_{0.5}$, in 5 of 8 trials at $\lambda_{0.75}$, in 1 of 8 trials at $\lambda_{1.25}$, and in 4 of 4 trials at $\lambda_{1.75}$ (Table 3). It appears that W_{ms} approximates the mean swimming velocity well when no flow is induced in the tank, but the approximation is not as reliable when flow is induced. At high turbulence, the mean-shifted approximation appears good at $\lambda_{1.25}$ but fails to capture the swimming velocity distribution at $\lambda_{1.75}$.

An example of larval velocity distributions in increasing turbulence levels (Fig. 4) demonstrates this disagreement between the 2 approaches. From top to bottom, each set of 3 panels represents velocity distributions at λ_0, $\lambda_{0.75}$, and $\lambda_{1.75}$, respectively. For each turbulence level, panels illustrate distributions of absolute larval velocity (W_a), larval swimming velocity (W_s), and mean-shifted larval swimming velocity (W_{ms}), along with the velocity distribution of mean local flow in the annulus around each larva (W_f). The

Table 2. Variance ratio test for the mean-shifted swimming velocity w_{ms} versus the swimming velocity w_s. The null hypothesis states that $\sigma^2_{shift\ abs} = \sigma^2_{rel}$ while the alternate hypothesis states that these variances are not equal. Significance level is $\alpha = 0.05/4 = 0.0125$ (with Bonferroni correction); significant results are indicated in **bold**

Trial		df	F	95% CI on $\sigma^2_{shift\ abs}/\sigma^2_{rel}$	p-value
OY5 λ_0	T1	54	1.76	[1.00, 2.96]	0.04
	T2	223	1.18	[0.91, 1.53]	0.21
	T3	137	1.15	[0.82, 1.61]	0.40
	T4	125	1.15	[0.82, 1.63]	0.43
$\lambda_{0.25}$	T1	112	1.29	[0.89, 1.88]	0.16
	T2	203	1.73	[1.31, 2.29]	**<0.001**
	T3	212	2.17	[1.66, 2.85]	**<0.001**
	T4	179	1.94	[1.44, 2.60]	**<0.001**
$\lambda_{0.5}$	T1	100	9.57	[6.45, 14.20]	**<0.001**
	T2	417	7.47	[6.16, 9.05]	**<0.001**
	T3	330	6.31	[5.08, 7.82]	**<0.001**
	T4	260	6.99	[5.48, 8.92]	**<0.001**
$\lambda_{0.75}$	T1	532	4.73	[3.99, 5.61]	**<0.001**
	T2	705	6.44	[5.55, 7.46]	**<0.001**
	T3	587	6.24	[5.31, 7.34]	**<0.001**
	T4	527	6.23	[5.25, 7.39]	**<0.001**
$\lambda_{1.25}$	T1	390	7.61	[6.23, 9.28]	**<0.001**
	T2	591	8.24	[7.01, 9.68]	**<0.001**
	T3	375	10.51	[8.58, 12.87]	**<0.001**
	T4	528	11.22	[9.46, 13.31]	**<0.001**
OY6 λ_0	T1	137	1.18	[0.84, 1.65]	0.33
	T2	366	1.43	[1.16, 1.75]	**<0.001**
	T3	195	1.59	[1.20, 2.11]	**0.001**
	T4	167	1.94	[1.43, 2.63]	**<0.001**
$\lambda_{0.25}$	T1	159	1.86	[1.36, 2.54]	**<0.001**
	T2	122	3.07	[2.15, 4.39]	**<0.001**
	T3	172	2.76	[2.05, 3.73]	**<0.001**
	T4	215	3.35	[2.57, 4.39]	**<0.001**
$\lambda_{0.5}$	T1	453	8.05	[6.69, 9.68]	**<0.001**
	T2	465	7.35	[6.12, 8.82]	**<0.001**
	T3	282	7.68	[6.08, 9.71]	**<0.001**
	T4	241	6.48	[5.03, 8.35]	**<0.001**
$\lambda_{0.75}$	T1	560	7.22	[6.12, 8.52]	**<0.001**
	T2	754	6.15	[5.33, 7.09]	**<0.001**
	T3	380	7.24	[5.92, 8.86]	**<0.001**
	T4	450	6.21	[5.16, 7.48]	**<0.001**
$\lambda_{1.25}$	T1	394	8.04	[6.23, 9.28]	**<0.001**
	T2	626	15.13	[7.01, 9.68]	**<0.001**
	T3	297	7.30	[8.58, 12.87]	**<0.001**
	T4	193	9.72	[9.46, 13.31]	**<0.001**
$\lambda_{1.75}$	T1	281	4.17	[3.30, 5.27]	**<0.001**
	T2	474	6.13	[5.12, 7.34]	**<0.001**
	T3	324	5.44	[4.37, 6.77]	**<0.001**
	T4	91	4.96	[3.28, 7.51]	**<0.001**

Table 3. Modified t-test for the mean-shifted swimming velocity w_{ms} versus the swimming velocity w_s. The null hypothesis states that $\mu_{shift\ abs} = \mu_{rel}$ while the alternate hypothesis states that these means are not equal. Significance level is $\sigma = 0.05/4 = 0.0125$ (with Bonferroni correction); significant results are in **bold**

Trial		df	t	95% CI on $\lvert\mu_{shift\ abs} - \mu_{rel}\rvert$	p–value
OY5 λ_0	T1	100.84	−1.46	[−.09, 0.014]	0.15
	T2	442.97	−1.25	[−0.04, 0.008]	0.21
	T3	272.62	−0.81	[−0.04, 0.014]	0.42
	T4	248.78	−0.56	[−0.03, 0.02]	0.58
$\lambda_{0.25}$	T1	220.28	−0.45	[−0.06, 0.03]	0.65
	T2	378.45	−0.22	[−0.04, 0.03]	0.82
	T3	372.83	−2.64	[−0.06, −0.009]	**0.008**
	T4	324.79	−2.19	[−0.06, −0.003]	0.02
$\lambda_{0.5}$	T1	120.65	0.06	[−0.10, 0.11]	0.95
	T2	526.62	−2.90	[−0.10, −0.02]	**0.004**
	T3	432.73	−4.70	[−0.15, −0.06]	**<0.001**
	T4	332.86	−1.57	[−0.10, 0.011]	0.12
$\lambda_{0.75}$	T1	747.14	−0.009	[−0.04, 0.04]	0.99
	T2	918.72	−0.67	[−0.06, 0.02]	0.50
	T3	770.23	−5.28	[−0.18, −0.08]	**<0.001**
	T4	691.81	−4.63	[−0.17, −0.07]	**<0.001**
$\lambda_{1.25}$	T1	490.73	1.38	[−0.02, 0.16]	0.17
	T2	732.30	−3.69	[−0.24, −0.07]	**<0.001**
	T3	445.69	−0.66	[−0.15, 0.07]	0.51
	T4	621.33	−0.88	[−0.15, 0.05]	0.38
OY6 λ_0	T1	272.14	−0.17	[−0.05, 0.04]	0.87
	T2	709.83	−1.98	[−0.04, −0.0001]	0.04
	T3	370.74	−0.74	[−0.04, 0.02]	0.46
	T4	302.96	1.44	[−0.008, 0.05]	0.15
$\lambda_{0.25}$	T1	291.61	−0.17	[−0.04, 0.03]	0.86
	T2	193.73	−0.06	[−0.05, 0.05]	0.95
	T3	282.08	−0.70	[−0.05, 0.02]	0.49
	T4	332.73	−2.89	[−0.09, −0.02]	**0.004**
$\lambda_{0.5}$	T1	563.81	−4.47	[−0.14, −0.05]	**<0.001**
	T2	589.17	−0.05	[−0.03, 0.04]	0.95
	T3	354.14	0.25	[−0.04, 0.06]	0.80
	T4	313.60	0.54	[−0.03, 0.06]	0.59
$\lambda_{0.75}$	T1	712.11	−2.57	[−0.12, −0.02]	**0.01**
	T2	992.88	−1.53	[−0.07, −0.009]	0.13
	T3	482.95	−2.66	[−0.13, −0.02]	**0.008**
	T4	591.18	−5.96	[−0.21, −0.11]	**<0.001**
$\lambda_{1.25}$	T1	490.46	1.50	[−0.02, 0.16]	0.15
	T2	708.37	1.87	[−0.004, 0.18]	0.06
	T3	376.92	−0.59	[−0.15, 0.08]	0.55
	T4	232.27	−1.66	[−0.24, 0.02]	0.09
$\lambda_{1.75}$	T1	408.30	13.25	[0.67, 0.90]	**<0.001**
	T2	624.57	18.71	[0.88, 1.10]	**<0.001**
	T3	439.12	9.13	[0.41, 0.63]	**<0.001**
	T4	126.23	6.34	[0.42, 0.81]	**<0.001**

results of the statistical analysis can be readily seen in comparisons of larval swimming velocity and mean-shifted swimming velocity: for still water (λ_0), the mean and variance of the 2 distributions are approximately equal (Fig. 4C), while for higher turbulence levels ($\lambda_{0.75}$ and $\lambda_{1.75}$), the variance in W_{ms} distribution is significantly larger than that of W_s (Fig. 4F,I). The means of these distributions in λ_0 and $\lambda_{0.75}$ appear roughly equal, but at $\lambda_{1.75}$, W_{ms} is centered far to the right of W_s.

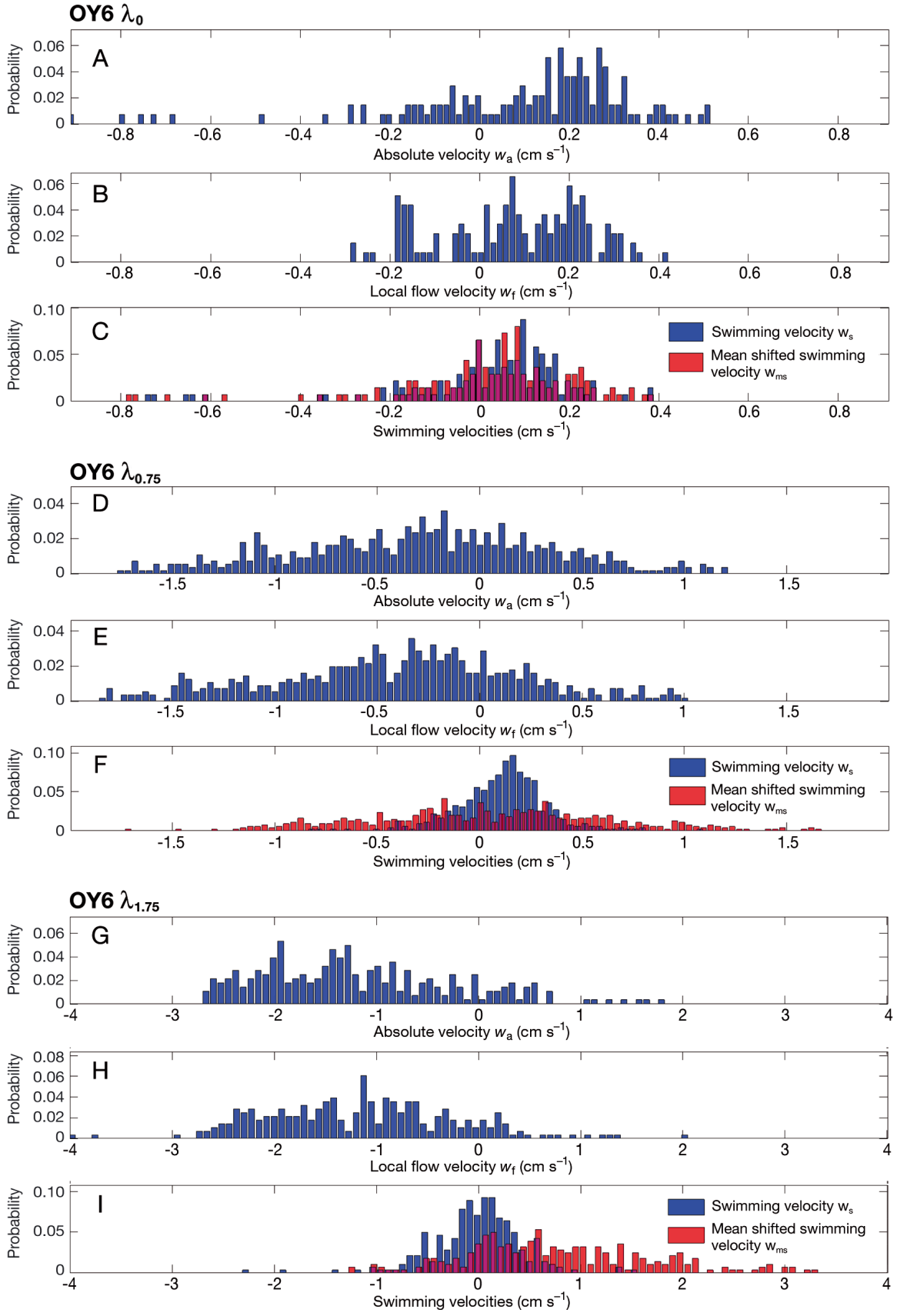

Fig. 4. Comparison of vertical instantaneous larval and flow velocity distributions for turbulence levels λ_0, $\lambda_{0.75}$, and $\lambda_{1.75}$. For each level, the top panel (A,D,G) illustrates mean absolute velocities, the middle panel (B,E,H) illustrates mean flow velocities in an annulus around each larva, and the bottom panel (C,F,I) shows mean swimming velocity, computed by subtracting the local flow around each larva from the absolute velocity (blue), and mean-shifted swimming velocity (red). (Where bars overlap they appear purple.) Turbulence levels have separate horizontal axis scaling for clarity

Table 4. Two-way ANOVA comparing the effects of turbulence level versus treatment order on larval swimming velocity. The null hypotheses state that average larval swimming velocities are equal across turbulence levels and independent of treatment order, while the alternate hypotheses state that these factors change average larval swimming velocity. Significance level is $\alpha = 0.05$; significant results are in **bold**

Source	SS	df	MS	*F*	p
OY5					
Turbulence level	0.043	4	0.010	5.67	**0.008**
Treatment order	0.001	3	<0.001	0.24	0.866
Error	0.022	12	0.002		
Total	0.067	19			
OY6					
Turbulence level	0.01	5	0.002	0.37	0.864
Treatment order	0.009	3	0.003	0.55	0.656
Error	0.079	15	0.005		
Total	0.097	23			

Vertical swimming velocity in turbulence

In OY5, larvae showed a significant swimming response to turbulence in the 2-way ANOVA (Table 4), swimming upward on average at higher turbulence levels. The post hoc multiple comparison test (Fig. 5) demonstrated that upward larval swimming increased significantly in moderate turbulence ($\lambda_{0.5}$ and $\lambda_{0.75}$) when compared with swimming in still water and at low turbulence (λ_0 and $\lambda_{0.25}$). Further, the *t*-tests (Table 5, Fig. 5) demonstrated that swimming velocities in moderate to high turbulence ($\lambda_{0.75}$ and $\lambda_{1.25}$) were significantly greater than zero. Treatment order had no effect on swimming velocity in either OY5 or OY6 (Table 4), indicating that exposure history did not influence the larval response to a particular treatment level.

OY6 data had greater inter-trial variability and no significant swimming response to turbulence was detected (Table 4), but several general patterns emerged in both experiments (dotted lines, Fig. 5). In almost all the trials, larval swimming velocities were near zero in low turbulence (λ_0 and $\lambda_{0.25}$), with both positive and negative mean velocities observed. At higher turbulence levels ($\lambda_{0.5}$ and higher), mean swimming velocities were greater in magnitude, and predominantly positive (upward swimming). At the highest turbulence level ($\lambda_{1.75}$, OY6), larvae demonstrated more flexibility in their vertical directionality, with larvae swimming upward in 2 trials and downward in 2 others.

Dive frequency in turbulence

Dive frequency (Fig. 6, Table 6) changed significantly with turbulence level in both OY5 and OY6. The χ^2 binomial comparison test on the contingency table (Table 6) gave df = 4, $\chi_Y^2 = 150.49$, and $p < 0.001$ for OY5 data, and df = 4, $\chi_Y^2 = 138.19$, and $p < 0.001$ for OY6 data. Dive frequency decreased with increasing turbulence level, where a subdivision of the contingency table demonstrated that the onset of statistically significant changes in dive frequency

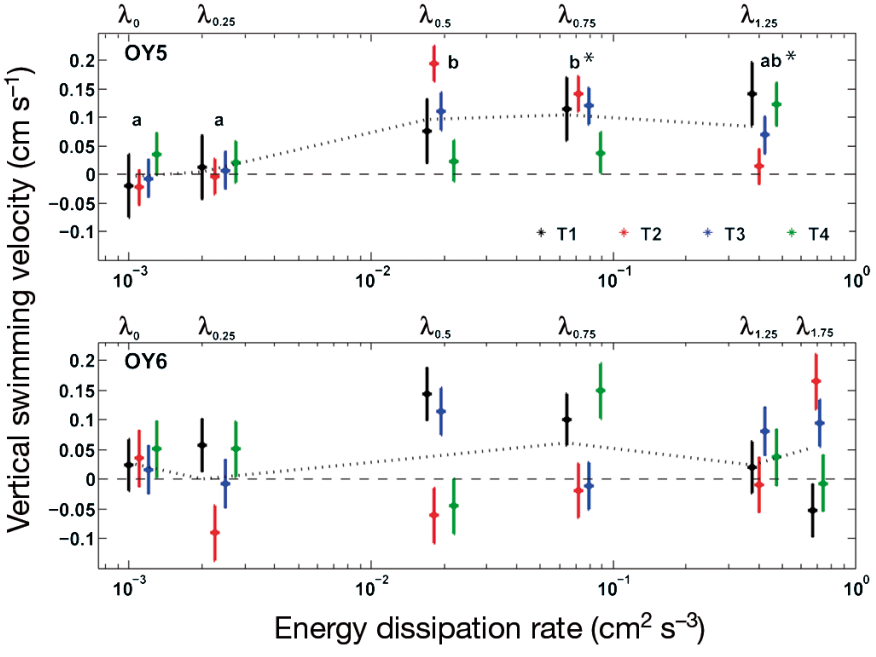

Fig. 5. Mean instantaneous swimming velocity w_s with respect to energy dissipation rate ε, for all 4 trials of both OY5 and OY6. Error bars are 95% confidence intervals as computed from pooled sample variance for each trial, and the dashed line indicates zero swimming velocity. Letters denote turbulence levels for which swimming velocities differ significantly, from the post hoc multiple comparison test. Asterisks above grouped trials denote significantly positive (upward) swimming velocities, as determined by *t*-tests (Table 5). Dotted lines indicate grouped trial means, to illustrate qualitative similarities between experiments OY5 and OY6

Table 5. Results of *t*-tests on OY5 data to determine the effects of turbulence level on upward larval swimming. Trials are grouped in each turbulence level and the null hypothesis states that the mean vertical larval swimming velocity is less than or equal to zero, and the alternate hypothesis states that it is positive (i.e. larvae swim upwards). Significance level is $\alpha = 0.05/5 = 0.01$ (with Bonferroni correction); significant results are in **bold**

Turbulence level	df	*t*	95% CI on $\lvert\mu_1-\mu_2\rvert$	p-value
λ_0	3	−0.23	[−0.06, 0.05]	0.58
$\lambda_{0.25}$	3	0.94	[−0.01, 0.02]	0.20
$\lambda_{0.5}$	3	2.94	[−0.05, 0.24]	0.03
$\lambda_{0.75}$	3	4.91	[0.01, 0.19]	**0.008**
$\lambda_{1.25}$	3	4.63	[0.02, 0.16]	**0.009**

occurred between levels λ_0 and $\lambda_{0.25}$ in OY5 (df = 2, $\chi_Y^2 = 12.02$, $p < 0.001$), and between $\lambda_{0.25}$ and $\lambda_{0.5}$ in OY6 (df = 2, $\chi_Y^2 = 9.73$, $p = 0.002$).

DISCUSSION

Swimming behaviour of oyster larvae varied with turbulence level, but not in the way we had hypothesized. Larval swimming velocities were weak in low turbulence and generally became stronger and upward in moderate turbulence. While high inter-trial variation in one experiment (OY6) precluded a statistically significant effect of turbulence on larval swimming, both experiments demonstrated qualitatively similar patterns. Upward swimming did not cease at an upper turbulence threshold. The dive response did not increase in frequency with increasing turbulence and did not cause downward movement of the population as a whole. In fact, the dive response in larvae decreased significantly in increasing turbulence, so our initial hypothesis of increasing turbulence as a dive trigger is not supported by the results. Larvae demonstrated the ability to maintain upward swimming velocities even in high turbulence, but the behaviour demonstrated some variability as average downward swimming was also observed at the highest turbulence level tested.

Table 6. Contingency table for χ^2 binomial comparison test for significance of dive frequency. Columns under turbulence levels contain the number of larval trajectories containing dives and the number of tracks not containing dives. The null hypothesis states that the proportion of larvae which dive (compared with non-divers) is independent of turbulence level, while the alternate hypothesis states that said proportion changes with turbulence level. Significance level is $\alpha = 0.05$

	Turbulence level					
	λ_0	$\lambda_{0.25}$	$\lambda_{0.5}$	$\lambda_{0.75}$	$\lambda_{1.25}$	$\lambda_{1.75}$
OY5						
Dive	24	8	7	4	1	–
No dive	666	893	1274	2893	3620	–
OY6						
Dive	23	17	10	5	1	0
No dive	1058	797	1640	2578	2726	3604

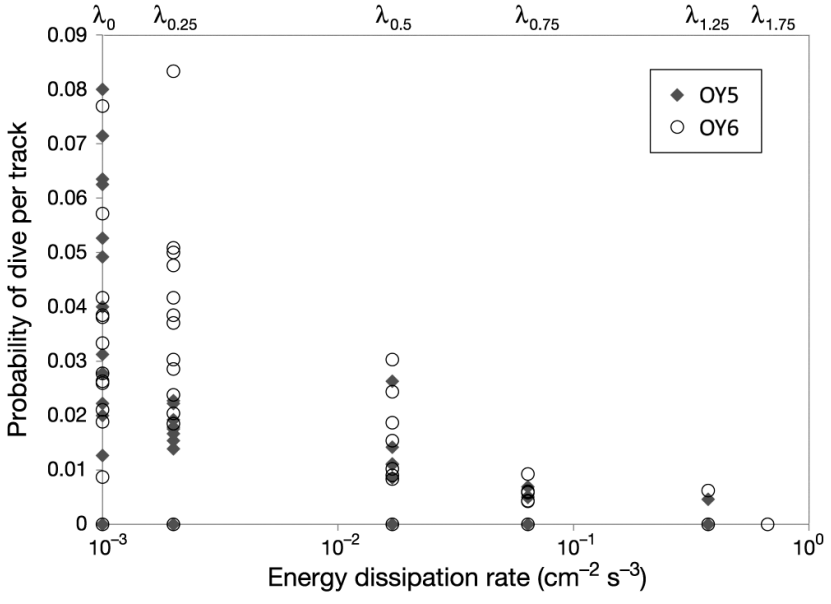

Fig. 6. Probability of dive (frequency of dives divided by number of larval trajectories) with respect to energy dissipation rate for each data set, where OY5 data sets are represented by a grey diamond, and OY6 data sets are represented by an open circle

We further found that simultaneous subtraction of local flow from larval movement was necessary to isolate larval behaviour, insofar as a mean-shifted larval velocity distribution could not reliably capture the mean and variance of the more accurate swimming velocity distribution. That is, a temporally and spatially averaged flow velocity does not adequately approximate local flow subtraction near individual larvae, confirming the necessity of a PIV-type approach to simultaneous larval tracking and flow quantification. This result has considerable implications for the design of larval behaviour experiments.

A surprising result of our experiments is the observation of continued larval

swimming even in highly turbulent flow. We expected larvae to cease swimming in high turbulence, and exhibit negative velocities consistent with sinking (Fuchs et al. 2004). Instead, even in high turbulence, larvae typically continued to swim upward. This suggests that turbulence may not be a settlement trigger for oyster larvae, given their tendency to swim up in highly turbulent flow. Further, the upward motion is an active response of larvae, and not a result of passive advection in turbulence. Studies of weakly inertial particle motion in turbulent flow demonstrate that turbulence leads to small modifications of the average fall velocity (e.g. Davila & Hunt 2001, Balachandar 2009, Balachandar & Eaton 2010), but does not cause the particles to move upward on average.

Another unexpected result of our experiments is the unwillingness or inability of larvae to dive in even moderately turbulent flows. The dive response is not uncommon when no flow is induced in the tank; it appears in up to 8% of larval tracks in a trial (Fig. 6). However, the dive frequency decreases (and in the case of the OY5 experiment, significantly) when any flow is induced in the tank.

The propensity of larvae to actively swim upward in high turbulence and not exhibit a dive response is especially interesting in the context of the results of Finelli & Wethey (2003). In an open-channel flow, they observed a dive response in approximately 4% of larvae filmed near a bottom boundary layer. Working with their reported shear velocity, camera height, and water level height, we estimated an energy dissipation rate of $\varepsilon \approx 0.37$ cm^2 s^{-3}, following the methodology of Fuchs et al. (2007). This dissipation rate is comparable to $\lambda_{1.25}$ from our experiment, where we observed only 2 dives in 6348 larval tracks. This wide discrepancy in dive frequency suggests the existence of a physical trigger for the dive response present in a channel flow that was absent in our experiment. Though estimated dissipation rates were comparable between their experiment and $\lambda_{1.25}$ of our experiment, their flume tank had a horizontal mean flow of 4.5 cm s^{-1}. The presence of a relatively large horizontal mean flow indicates strong vertical shear approaching the bottom of the flume, suggesting that larvae may dive in response to vertical shear. Alternately, the presence of the vertical mean flows in the grid-stirred tank at higher turbulence levels may have suppressed the larval dive response, as larvae may have chosen to swim against a downward mean flow to maintain vertical position (observed experimentally for cyprid larvae in DiBacco et al. 2011). Larval swimming and diving responses to local components of turbulence that they may sense (acceleration, strain, and vorticity) are a subject of current investigation.

Oyster larvae continued to swim upward in turbulent flow of energy dissipation rates comparable to estuarine and calm surf zone conditions. If turbulence is a trigger to settlement, we have yet to observe a threshold turbulent energy level high enough to cause these larvae to consistently stop swimming and sink or dive out of the water column. Further experiments with more strongly turbulent flows within reasonable field conditions may yet yield this threshold. It is also possible that turbulence induced by vertical grid movement is insufficient to trigger a settlement or downward swimming response in competent larvae, though downward swimming has been reported for larger competent larvae in a turbulence tank study (Fuchs et al. 2013). Our larvae were in an early phase of competency, as they had not reached the larger sizes (~300 µm) of settling larvae reported from other studies (e.g. Galtsoff 1964). Larger larvae may be more inclined to move downward as they develop heavier shells towards the end of competency, due to either energetic constraints (more energy needed to keep the shell aloft) or developmental limits (i.e. they become desperate larvae; Knight-Jones 1953). Further, the specific turbulent cues to which larvae respond are not yet well understood; larvae approaching nearshore environments may react to highly turbulent flows with strong shear (as in the flume of Finelli & Wethey 2003), or a combination of turbulence and a chemical cue may be required to induce larval settlement responses (see for instance Hadfield & Koehl 2007, Koehl & Hadfield 2010). Our results raise the intriguing question of how larval responses to turbulent flows may change through the competent-to-settle period.

A useful technical result obtained from this study is the demonstration that adjusting absolute larval velocity distributions by subtracting mean, non-local flow appears to be inadequate for capturing larval swimming metrics, especially the variances of swimming velocity distributions. The variances in the mean-shifted swimming velocity distributions increased dramatically with increasing turbulence level, likely due to enhanced random variability in the experimental flow. A similar increase in variance was also observed in Fuchs et al. (2004), although their mean flow subtraction methodology differed somewhat from that presented here. Our mean flow velocities were considerably greater than those reported in Fuchs et al. (2004), as they observed maximal mean flows of −0.7 cm s^{-1}, while ours were −2.6 cm s^{-1}, though this discrepancy may be due to the time inter-

val over which the mean flow was calculated. Roy et al. (2012) also reported sporadic considerable mean flows in their tank, occurring at far lower turbulence levels than used in our experiment. Mean flows appear inherent to the vertically oscillating grid tank design, and as the mean-shifted velocity correction was especially inaccurate at high turbulence, we conclude that local flow subtraction is an unavoidable necessity at high turbulence. The spatial and temporal gradients in flow velocity at high turbulence also impede efforts to separate average flow from larval swimming velocities, further indicating the necessity of local flow subtraction. Finally, flow subtraction is necessary to identify behaviours such as the dive response, as they occur on an individual level and are too transient to be observed clearly in swimming velocity distributions at all but the lowest turbulence levels (e.g. Fig. 4C). To determine how often the diving behavior occurs, however, one requires the isolated swimming velocity time series of each individual larva.

In this study, we determined that oyster larvae, unlike larvae of previously studied mollusc species, do not sink in experimental turbulent flows comparable to coastal settlement zones, and in fact continue to actively swim. Further, we found that previous methods for estimating larval swimming velocities may be inadequate to distinguish behaviour from advection in fluid flow. Because larval behaviour may have profound effects on supply and successful settlement to the benthos, we must continue to carefully isolate behavioural effects from flow in larval invertebrates. For oyster larvae specifically, further work remains to determine a potential settlement response to hydrodynamic cues. Larval swimming responses to faster flows, vertical shear, and combined turbulent and chemical cues are the subject of future investigation.

Acknowledgements. Thanks to Skylar Bayer, Meredith White, and Stace Beaulieu for discussions of larval behaviour and culture; Susan Mills for larval acquisition and culture, and experimental assistance; Shawn Arellano for discussions of larval tracking and behaviour in flow; and Heidi Fuchs for helpful discussions during the inception of the project. Thanks also to Joseph Fitzgerald for discussions of larval behaviour, tracking, and data analysis; Vicke Starczak for suggestions on statistical analysis; and three anonymous reviewers for helpful manuscript comments and suggestions. We gratefully acknowledge the culturing expertise of the Aquaculture Research Facility in Dennis, MA, who supplied the larval oysters used in this study. This work was supported by NSF grant OCE-0850419, grants from WHOI Coastal Ocean Institute, discretionary WHOI funds to purchase the infrared laser and high-speed camera, and a WHOI Ocean Life Fellowship to L.S.M.

LITERATURE CITED

Balachandar S (2009) A scaling analysis for point-particle approaches to turbulent multiphase flows. Int J Multiph Flow 35:801–810

Balachandar S, Eaton J (2010) Turbulent dispersed multiphase flow. Annu Rev Fluid Mech 42:111–133

Butman C (1987) Larval settlement of soft-sediment invertebrates: the spatial scales of pattern explained by active habitat selection and the emerging role of hydrodynamical processes. Oceanogr Mar Biol Annu Rev 25:113–165

Butman C, Grassle J, Webb C (1988) Substrate choices made by marine larvae settling in still water and in a flume flow. Nature 333:771–773

Clay TW, Grünbaum D (2010) Morphology–flow interactions lead to stage-selective vertical transport of larval sand dollars in shear flow. J Exp Biol 213:1281–1292

Davila J, Hunt J (2001) Settling of small particles near vortices and in turbulence. J Fluid Mech 440:117–145

Dekshenieks MM, Hofmann EE, Klinck JM, Powell EN (1996) Modeling the vertical distribution of oyster larvae in response to environmental conditions. Mar Ecol Prog Ser 136:97–110

DiBacco C, Fuchs HL, Pineda J, Helfrich K (2011) Swimming behavior and velocities of barnacle cyprids in a downwelling flume. Mar Ecol Prog Ser 433:131–148

Doron P, Bertuccioli L, Katz J, Osborn T (2001) Turbulence characteristics and dissipation estimates in the coastal ocean bottom boundary layer from PIV data. J Phys Oceanogr 31:2108–2134

Finelli C, Wethey D (2003) Behavior of oyster (*Crassostrea virginica*) larvae in flume boundary layer flows. Mar Biol 143:703–711

Fuchs HL, Mullineaux LS, Solow A (2004) Sinking behavior of gastropod larvae (*Ilyanassa obsoleta*) in turbulence. Limnol Oceanogr 49:1937–1948

Fuchs HL, Neubert MG, Mullineaux LS (2007) Effects of turbulence-mediated settlement behaviour on larval supply and settlement in tidal currents. Limnol Oceanogr 52: 1156–1165

Fuchs HL, Huter EJ, Schmitt EL, Guazzo RA (2013) Active downward propulsion by oyster larvae in turbulence. J Exp Biol 216:1458–1469

Galtsoff PS (1964) The American oyster *Crassostrea virginica* (Gmelin). US Fish Wildl Serv Fish Bull 64:1–480

George R, Flick R, Guza R (1994) Observations of turbulence in the surf zone. J Geophys Res 99:801–810

Glass G, Peckham P, Sanders J (1972) Consequences of failure to meet assumptions underlying the fixed effects analyses of variance and covariance. Rev Educ Res 42: 237–288

Gross T, Nowell A (1985) Spectral scaling in a tidal boundary layer. J Phys Oceanogr 15:496–508

Hadfield MG, Koehl MAR (2004) Rapid behavioral responses of an invertebrate larva to dissolved settlement cue. Biol Bull 207:28–43

Helfrich KR, Pineda J (2003) Accumulation of particles in propagating fronts. Limnol Oceanogr 48:1509–1520

Hidu H, Haskin H (1978) Swimming speeds of oyster larvae *Crassostrea virginica* in different salinities and temperatures. Estuar Coast 1:252–255

Kennedy VS (1986) Expected seasonal presence of *Crassostrea virginica* (Gmelin) larval populations, emphasizing Chesapeake Bay. Am Malacol Bull, Spec Edn 3: 25–29

Kennedy VS (1996) Biology of larvae and spat. In: Kennedy VS, Newell RIE, Eble AF (eds) The eastern oyster (*Crassostrea virginica*). Maryland Sea Grant, College Park, MD, p 371–411

Kim C, Park K, Powers S, Graham W, Bayha K (2010) Oyster larval transport in coastal Alabama: dominance of physical transport over biological behavior in a shallow estuary. J Geophys Res 115(C10):C10019, doi:10.1029/2010JC006115

Knight-Jones EW (1953) Laboratory experiments on gregariousness during setting in *Balanus balanoides* and other barnacles. J Exp Biol 30:584–599

Koehl MAR, Hadfield MG (2010) Hydrodynamics of larval settlement from a larval point of view. Integr Comp Biol 50:539–551

Koehl MAR, Reidenbach MA (2007) Swimming by microscopic organisms in ambient water flow. Exp Fluids 43: 755–768

McCulloch A, Shanks AL (2003) Topographically generated fronts, very nearshore oceanography and the distribution and settlement of mussel larvae and barnacle cyprids. J Plankton Res 25:1427–1439

McDonald KA (2012) Earliest ciliary swimming effects vertical transport of planktonic embryos in turbulence and shear flow. J Exp Biol 215:141–151

Metaxas A (2001) Behaviour in flow: perspectives on the distribution and dispersion of meroplanktonic larvae in the water column. Can J Fish Aquat Sci 58:86–98

North EW, Schlag Z, Hood RR, Li M, Zhong L, Gross T, Kennedy VS (2008) Vertical swimming behavior influences the dispersal of simulated oyster larvae in a coupled particle-tracking and hydrodynamic model of Chesapeake Bay. Mar Ecol Prog Ser 359:99–115

Raffel M, Willert C, Kompenhans J (1998) Particle image velocimetry: a practical guide. Springer-Verlag, Berlin

Roy A, Metaxas A, Ross T (2012) Swimming patterns of larval *Strongylocentrotus droebachiensis* in turbulence in the laboratory. Mar Ecol Prog Ser 453:117–127

Scotti A, Pineda J (2007) Plankton accumulation and transport in propagating nonlinear internal fronts. J Mar Res 65:117–145

Shanks AL, Brink L (2005) Upwelling, downwelling, and cross-shelf transport of bivalve larvae: test of a hypothesis. Mar Ecol Prog Ser 302:1–12

Shanks AL, McCulloch A, Miller J (2003) Topographically generated fronts, very nearshore oceanography and the distribution of larval invertebrates and holoplankters. J Plankton Res 25:1251–1277

Tamburri M, Finelli C, Wethey D, Zimmer-Faust R (1996) Chemical induction of larval settlement behavior in flow. Biol Bull 191:367–373

Thompson R, Newell RIE, Kennedy VS, Mann R (1996) Reproductive processes and early development. In: Kennedy VS, Newell RIE, Eble AF (eds) The eastern oyster (*Crassostrea virginica*). Maryland Sea Grant, College Park, MD, p 335–364

Whitman ER, Reidenbach MA (2012) Benthic flow environments affect recruitment of *Crassostrea virginica* larvae to an intertidal oyster reef. Mar Ecol Prog Ser 463: 177–191

Woodson CB, McManus MA, Tyburczy JA, Barth JA and others (2012) Coastal fronts set recruitment and connectivity pattern across multiple taxa. Limnol Oceanogr 57: 582–596

Yates F (1934) Contingency tables involving small numbers and the χ^2 test. Suppl J R Stat Soc 1:217–235

Editorial responsibility: Steven Morgan, Bodega Bay, California, USA

Submitted: November 14, 2012; Accepted: April 22, 2013
Proofs received from author(s): July 9, 2013